

Bending, Twisting, and Breaking CuCN Chains to Produce Framework Materials: The Reactions of CuCN with Alkali-Metal Halides[†]

Ann M. Chippindale,^{*,‡} Simon J. Hibble,^{*,‡} and Andrew R. Cowley[§]

School of Chemistry, University of Reading, Whiteknights, Reading, Berks RG6 6AD, U.K., and Chemical Crystallography Laboratory, University of Oxford, 12 Mansfield Road, Oxford OX1 3TA, U.K.

Received July 22, 2004

The reactions of the low-temperature polymorph of copper(I) cyanide (LT-CuCN) with concentrated aqueous alkali-metal halide solutions have been investigated. At room temperature, KX (X = Br and I) and CsX (X = Cl, Br, and I) produce the addition products $K[Cu_2(CN)_2Br] \cdot H_2O$ (I), $K_3[Cu_6(CN)_6I_3] \cdot 2H_2O$ (II), $Cs[Cu_3(CN)_3Cl]$ (III), $Cs[Cu_3(CN)_3Br]$ (IV), and $Cs_2[Cu_4(CN)_4I_2] \cdot H_2O$ (V), with 3-D frameworks in which the $-(CuCN)-$ chains present in CuCN persist. No reaction occurs, however, with NaX (X = Cl, Br, I) or KCl. The addition compounds, I–V, revert to CuCN when washed. Both low- and high-temperature polymorphs of CuCN (LT- and HT-CuCN) are produced, except in the case of $Cs[Cu_3(CN)_3Cl]$ (III), which converts only to LT-CuCN. Heating similar AX–CuCN reaction mixtures under hydrothermal conditions at 453 K for 1 day produces single crystals of I–V suitable for structure determination. Under these more forcing conditions, reactions also occur with NaX (X = Cl, Br, I) and KCl. NaBr and KCl cause some conversion of LT-CuCN into HT-CuCN, while NaCl and NaI, respectively, react to form the mixed-valence Cu(I)/Cu(II) compounds $[Cu^{II}(OH_2)_4][Cu^I_4(CN)_6]$, a known phase, and $[Cu^{II}(OH_2)_4][Cu^I_4(CN)_4I_2]$ (VI), a 3-D framework, which contains infinite $-(CuCN)-$ chains. After 3 days of heating under hydrothermal conditions, the reaction between KI and CuCN produces $[Cu^{II}(OH_2)_4][Cu^I_2(CN)I_2]_2$ (VII), in which the CuCN chains are broken into single Cu–CN–Cu units, which in turn are linked into chains via iodine atoms and then into layers via long Cu–C and Cu–Cu interactions.

Introduction

The construction of complex materials by the joining of simple identifiable units is the way that organic chemistry proceeds. There are areas of inorganic chemistry, for example, coordination chemistry, where this is also the case. However, in traditional solid-state chemistry, materials are normally produced at high temperature, and the high degree of bond breaking and making during reaction is such that all trace of the identity of the units present in the starting materials is lost. Producing solids at lower temperatures means that it is more likely that the species present in the precursors will retain some degree of integrity in the final product. When this degree of retained integrity is very high, the chemistry is claimed to be supramolecular, although this term is also used for the construction of species in solution.

It is not entirely clear when solid-state chemistry becomes supramolecular; for example, microporous solids can be envisaged as constructed from simpler building blocks that might exist in solution as precursors. This has shown to be a valid hypothesis in a number of cases, e.g., in the assembly of microporous metal phosphates.^{1,2}

Recently, there has been renewed interest in the chemistry of metal cyanides, particularly in oligonuclear complexes,³ which present possibilities for realizing molecular magnets^{4,5} and interesting redox behavior,³ as well as in the construction of supramolecular compounds,^{6,7} which may exhibit porosity.^{8,9} Both these fields make use of the fact that $C \equiv N$ groups

* To whom correspondence should be addressed. E-mail: a.m.chippindale@rdg.ac.uk (A.M.C.); s.j.hibble@rdg.ac.uk (S.J.H.).

[†] Dedicated to Peter G. Dickens, our chemical father.

[‡] University of Reading.

[§] University of Oxford.

- (1) Vistad, O. B.; Akporiaye, D. E.; Taulelle, F.; Lillerud, K. P. *Chem. Mater.* **2003**, *15*, 1639.
- (2) Serre, C.; Taulelle, F.; Férey, G. *Chem. Commun.* **2003**, 2755.
- (3) Vahrenkamp, H.; Geiss, A.; Richardson, G. N. *J. Chem. Soc., Dalton Trans.* **1997**, 3643.
- (4) Zhang, S. W.; Fu, D. G.; Sun, W. Y.; Hu, Z.; Yu, K. B.; Tang, W. X. *Inorg. Chem.* **2000**, *39*, 1142 and references therein.
- (5) Ferlay, S.; Malleh, T.; Ouakès, R.; Veillet P.; Verdaguer, M. *Nature* **1995**, *378*, 701.

Table 1. Addition Compounds, AX–CuCN, Formed by Reaction of LT–CuCN with Aqueous Alkali-Metal Halide (AX) Solutions at Room Temperature, Their Infrared Bands in the C≡N Stretching Region, and the Products Formed on Reaction with Water

AX	AX–CuCN addition product	color of powder	IR stretching wavenumbers, $\nu_{\text{C}\equiv\text{N}}/\text{cm}^{-1}$	no. distinct C≡N groups	products formed on washing AX–CuCN
KBr	$\text{K}[\text{Cu}_2(\text{CN})_2\text{Br}] \cdot \text{H}_2\text{O}$ (I)	beige	2168(w), 2112(s)	1	LT-CuCN + HT-CuCN
KI	$\text{K}_3[\text{Cu}_6(\text{CN})_6\text{I}_3] \cdot 2\text{H}_2\text{O}$ (II)	pale yellow	2125(s), 2107(s), 2097(sh, s)	3	LT-CuCN + HT-CuCN
CsCl	$\text{Cs}[\text{Cu}_3(\text{CN})_3\text{Cl}]$ (III)	cream	2154(m), 2117(s)	1	LT-CuCN only
CsBr	$\text{Cs}[\text{Cu}_3(\text{CN})_3\text{Br}]$ (IV)	cream	2161(w), 2119(s)	1	LT-CuCN + HT-CuCN (trace)
CsI	$\text{Cs}_2[\text{Cu}_4(\text{CN})_4\text{I}_2] \cdot \text{H}_2\text{O}$ (V)	cream/v pale yellow	2154(broad, w), 2128(m), 2104(s), 2049(broad, w)	3	LT-CuCN + HT-CuCN

can form strong linkages between metal atoms. By employing different metals, a range of $\text{M}(\text{CN})_x$ units can be prepared, which in turn can be linked together to form supramolecular materials. Examples such as linear $[\text{Ag}(\text{CN})_2]^-$, tetrahedral $[\text{Zn}(\text{CN})_4]^{2-}$, square-planar $[\text{Ni}(\text{CN})_4]^{2-}$, and octahedral $[\text{Fe}(\text{CN})_6]^{4-}$ have been used as building blocks combining with themselves, other complex metal ions, or organic species, such as amines, to generate 1-, 2-, and 3-dimensional frameworks.^{6,7} Of relevance to this paper is the work of a number of groups who have used CuCN to prepare framework materials in the presence of amines,^{10–18} crown ethers,¹⁹ and cryptands.¹⁹ In many of these materials, infinite $-(\text{CuCN})-$ chains, long presumed to be present in CuCN, but only recently confirmed by our recent work,^{20,21} or portions of the $-(\text{CuCN})-$ chain, are retained in the products. Bowmaker et al. have also observed that CuCN will react even at room temperature with aqueous KBr and KI.¹⁶ We recently determined the structure of the product formed by reaction with KBr, $\text{K}[\text{Cu}_2(\text{CN})_2\text{Br}] \cdot \text{H}_2\text{O}$, and found it formed a zeolitic framework with infinite $-(\text{CuCN})-$ chains linked by bromine atoms with potassium ions in the cavities.²⁰ We also found that the infinite $-(\text{CuCN})-$ chains can self-assemble to form two different polymorphs of CuCN, the high temperature (HT-) and low temperature (LT-) forms, and that these forms can be interconverted via the KBr addition product.²⁰ In the present work, we have studied further the reactions of CuCN with alkali-metal

halides, both at room temperature and under hydrothermal conditions at 453 K, and report the structures of six new materials.

Experimental Section

Syntheses. Copper(I) cyanide as supplied by Aldrich was used in the syntheses. Powder X-ray diffraction showed that this was the low-temperature modification of CuCN (LT-CuCN). Caution should be exercised when handling copper cyanide or any of the cyanide containing products due to their toxicity.

Room-Temperature Reactions of CuCN with Aqueous Alkali-Metal Halides. The reactions of the low-temperature polymorph of copper(I) cyanide (LT-CuCN) with concentrated aqueous alkali-metal halide solutions were investigated. CuCN (0.4 g, ~4.5 mmol) was stirred at room temperature for 2 h with approximately 10 mmol of alkali-metal halide (NaX, KX, and CsX (X = Cl, Br, I)) in 10 mL of deionized water. The polycrystalline products were filtered and dried at room temperature and their powder X-ray diffraction patterns recorded.

In the cases of NaCl, NaBr, and KCl, the recovered products corresponded to unreacted LT-CuCN. For NaI, by far the major phase was LT-CuCN, with a very small amount of γ -CuI. For the remaining alkali-metal halides, KBr, KI, CsCl, CsBr, and CsI, changes in the turbidities and colors of the suspensions indicated that immediate reaction had taken place, although the mixtures were then stirred for 2 h to ensure complete reaction. The powder X-ray diffraction patterns of the dried polycrystalline products showed that no crystalline CuCN remained. Subsequent detailed analysis, making use of the structures determined below, showed that each pattern corresponded to a single AX–CuCN addition product (Table 1). In the case of the KI product, a small amount of γ -CuI was also visible in the pattern.

Reaction of the AX–CuCN Addition Products with Water. The effect of washing the KBr, KI, CsCl, CsBr, and CsI addition products, I–V, with copious amounts of water at room temperature was investigated. In all cases, CuCN was re-formed (Table 1). In the case of the CsCl addition product, III, only LT-CuCN was detectable by powder X-ray diffraction, but in all other cases, HT-CuCN was also found to be present. This demonstrates a gentle chemical method for converting LT-CuCN into HT-CuCN, a process which can also be achieved by heating LT-CuCN at 563 K.^{22,23}

Hydrothermal Reactions of CuCN with Aqueous Alkali-Metal Halides. Preparation of Single Crystals of the AX–CuCN Addition Products, I–V. Single crystals of the AX–CuCN addition products listed in Table 1 were obtained from LT-CuCN under hydrothermal conditions. Approximately 0.1 g of CuCN (1

- (6) Iwamoto, T. In *Comprehensive Supramolecular Chemistry*; MacNicol, D. D., Toda, F., Bishop, R., Eds.; Pergamon Press: Oxford, U.K., 1996; Vol. 6, Chapter 19, p 643.
- (7) Cernak, J.; Orendac, M.; Potocnak, I.; Chomic, J.; Orendacova, A.; Skorsepca, J.; Feher, A. *Coord. Chem. Rev.* **2002**, *224*, 51.
- (8) Ibrahim, A. M. M. *J. Organomet. Chem.* **1998**, *556*, 1.
- (9) Janiak, C. *Angew. Chem., Int. Ed. Engl.* **1997**, *36*, 1431.
- (10) Chesnut, D. J.; Plewak, D.; Zubieta, J. *J. Chem. Soc., Dalton Trans.* **2001**, 2567.
- (11) Chesnut, D. J.; Kusnetzow, A.; Birge, R.; Zubieta, J. *Inorg. Chem.* **1999**, *38*, 5484.
- (12) Chesnut, D. J.; Zubieta, J. *J. Chem. Commun.* **1998**, 1707.
- (13) Chesnut, D. J.; Kusnetzow, A.; Zubieta, J. *J. Chem. Soc., Dalton Trans.* **1998**, 4081.
- (14) Colacio, E.; Dominguez-Vera, J. M.; Lloret, F.; Moreno Sanchez, J. M.; Kivekas, R.; Rodriguez, A.; Sillanpaa, R. *Inorg. Chem.* **2003**, *42*, 4209.
- (15) Kromp, T.; Sheldrick, W. S.; Nather, C. *Z. Anorg. Allg. Chem.* **2003**, *629*, 2097 and references therein.
- (16) Bowmaker, G. A.; Hartl, H.; Urban, V. *Inorg. Chem.* **2000**, *39*, 4548.
- (17) Teichert, O.; Sheldrick, W. S. *Z. Anorg. Allg. Chem.* **2000**, *626*, 1509.
- (18) Pretsch, T.; Brudgam, I.; Hartl, H. *Z. Anorg. Allg. Chem.* **2003**, *629*, 942.
- (19) Muhle, J.; Sheldrick, W. S. *Z. Anorg. Allg. Chem.* **2003**, *629*, 2097.
- (20) Hibble, S. J.; Eversfield, S. G.; Cowley, A. R.; Chippindale, A. M. *Angew. Chem., Int. Ed.* **2004**, *43*, 628.
- (21) Hibble, S. J.; Cheyne, S. M.; Hannon, A. C.; Eversfield, S. G. *Inorg. Chem.* **2002**, *41*, 4990.

(22) Wang, J.; Collins, M. F.; Johari, G. P. *Phys. Rev. B* **2002**, *65*, article 180103.

(23) Reckeweg, O.; Lind, C.; Simon, A.; DiSalvo, F. J. *Z. Naturforsch., B: Chem Sci.* **2003**, *58*, 155.

Table 2. Crystallographic Data for Compounds **I–IV**

	K[Cu ₂ (CN) ₂ Br]·H ₂ O (I)	K ₃ [Cu ₆ (CN) ₆ I ₃]·2H ₂ O (II)	Cs[Cu ₃ (CN) ₃ Cl] (III)	Cs[Cu ₃ (CN) ₃ Br] (IV)
<i>M_r</i>	316.16	1071.45	437.07	481.52
cryst habit	colorless plate	colorless plate	colorless plate	colorless plate
dimensions/mm	0.01 × 0.08 × 0.10	0.02 × 0.10 × 0.20	0.02 × 0.10 × 0.22	0.02 × 0.08 × 0.08
cryst syst	orthorhombic	monoclinic	trigonal	trigonal
space group	<i>Pnma</i> (No. 62)	<i>C2/c</i> (No. 15)	<i>R3c</i> (No. 167)	<i>R3c</i> (No. 167)
<i>T/K</i>	293(2)	293(2)	293(2)	293(2)
<i>a/Å</i>	7.5522(4)	13.0622(4)	10.3041(4)	10.4610(5)
<i>b/Å</i>	10.4461(5)	13.1167(4)	10.3041(4)	10.4610(5)
<i>c/Å</i>	9.3825(5)	13.4592(4)	13.8470(7)	13.9820(5)
<i>α/deg</i>	90	90	90	90
<i>β/deg</i>	90	107.684(2)	90	90
<i>γ/deg</i>	90	90	120	120
<i>V/Å³</i>	740.2	2197.0	1273.2	1325.1
<i>Z</i>	4	4	6	6
wavelength/Å	0.71073	0.71073	0.71073	0.71073
<i>μ/mm⁻¹</i>	11.621	10.500	11.918	15.673
<i>D_{calc}/g cm⁻³</i>	2.819	3.227	3.420	3.621
<i>R(F); R_w(F)</i>	0.0293; 0.0331	0.0708; 0.0722	0.0292; 0.0320	0.0286; 0.0363

mmol) was added to 7 mmol of AX in 5 mL of water, and the mixture was heated in an autoclave at 453 K for 20 h. Crystals of compounds **I–VI**, suitable for diffraction studies, were picked from the supernatants. In the KI–CuCN case, it was necessary to wash the crystal with acetone to remove small adhering crystals of KI. The morphology of Cs[Cu₃(CN)₃Cl] (**III**) and Cs[Cu₃(CN)₃Br] (**IV**) is particularly interesting. Both occur as multiple twins forming hollow tubes of hexagonal cross section which cleave easily into platelike single crystals.

Preparation of Cu(I)/Cu(II) Mixed-Valence Compounds, VI and VII. Hydrothermal reactions using NaCl and NaI solutions, under the same heating conditions as described above, did not produce simple addition products, but instead produced complex mixtures containing mixed-valence materials. Purple crystals in the NaCl product mixture were identified, from the unit-cell parameters determined by single-crystal X-ray diffraction, as the known phase [Cu^{II}(OH₂)₄][Cu^I₄(CN)₆].¹¹ The reaction using NaI produced dark-green blocks of a new phase, [Cu^{II}(OH₂)₄][Cu^I₄(CN)₄I₂] (**VI**). Prolonged hydrothermal reaction of KI and CuCN for 3 days at 453 K gave dark-green blocks of [Cu^{II}(OH₂)₄][Cu^I₂(CN)I₂]₂ (**VII**) as the major phase. The structures of **VI** and **VII** were determined by single-crystal X-ray diffraction from crystals picked from the mixtures.

Recrystallization of CuCN under Hydrothermal Conditions. Similar hydrothermal reactions were undertaken for NaBr and KCl to determine whether these alkali-metal halides react with CuCN under conditions more forcing than stirring at room temperature. In these reactions, the only crystalline products were LT- and HT-CuCN, as identified by powder X-ray diffraction.

Crystal Structure Determination. X-ray intensity data were collected at room temperature for compounds **I–VII** using a Nonius KappaCCD diffractometer (graphite-monochromated Mo K α radiation). Data sets were processed using DENZO²⁴ and SCALEPACK.²⁵ Full crystallographic details are given in Tables 2 and 3.

The structures of **II–VII** were solved by direct methods using the program SIR92²⁶ and all nonhydrogen framework and non-framework atoms located. Subsequent Fourier calculations and least-

Table 3. Crystallographic Data for Compounds **V–VII**

	Cs ₂ [Cu ₄ (CN) ₄ -I ₂]·H ₂ O (V)	[Cu(H ₂ O) ₄][Cu ₄ (CN) ₄ I ₂] (VI)	[Cu(H ₂ O) ₄][Cu ₂ (CN)I ₂] ₂ (VII)
<i>M_r</i>	895.90	747.69	949.45
cryst habit	colorless plate	green block	green block
dimensions/mm	0.01 × 0.10 × 0.20	0.08 × 0.10 × 0.14	0.08 × 0.10 × 0.10
cryst syst	monoclinic	monoclinic	triclinic
space group	<i>C2/c</i> (No. 15)	<i>P2₁/c</i> (No. 14)	<i>P1</i> (No. 2)
<i>T/K</i>	293(2)	293(2)	293(2)
<i>a/Å</i>	8.9865(4)	7.0605(3)	7.1656(2)
<i>b/Å</i>	10.9970(5)	15.8917(7)	7.2939(2)
<i>c/Å</i>	15.9847(7)	7.5392(3)	8.7309(3)
<i>α/deg</i>	90	90	79.440(2)
<i>β/deg</i>	92.423(2)	96.500(2)	80.334(2)
<i>γ/deg</i>	90	90	73.150(2)
<i>V/Å³</i>	1578.3	840.5	426.1
<i>Z</i>	4	2	1
wavelength/Å	0.71073	0.71073	0.71073
<i>μ/mm⁻¹</i>	13.761	9.904	13.380
<i>D_{calc}/g cm⁻³</i>	3.768	2.954	3.700
<i>R(F); R_w(F)</i>	0.0468; 0.0563	0.0400; 0.0476	0.0327; 0.0405

squares refinements on *F* were carried out using the CRYSTALS suite of programs.²⁷ The structure of **I** at 150 K has been reported previously²⁰ and was used as the starting model for the room-temperature structure described here.

With the exception of K₃[Cu₆(CN)₆I₃]·2H₂O (**II**), all the crystals were of high quality, and the refinements proceeded smoothly. K₃[Cu₆(CN)₆I₃]·2H₂O was, however, found to be twinned, and a paucity of data led to a rather poor *R* factor. Several of the structures contain nonframework water molecules located either close to alkali-metal cations or, for the mixed-valence compounds, as part of the complex ion [Cu^{II}(OH₂)₄]²⁺. The hydrogen atoms of the water molecules were located in difference Fourier maps for [Cu(OH₂)₄]-[Cu₄(CN)₄I₂] (**VI**) and [Cu(OH₂)₄][Cu₂(CN)I₂]₂ (**VII**) but could not be found in K[Cu₂(CN)₂Br]·H₂O (**I**), K₃[Cu₆(CN)₆I₃]·2H₂O (**II**), and Cs₂[Cu₄(CN)₄I₂]·H₂O (**V**).

A frequently occurring problem for cyanide-containing compounds is the determination of the orientation of the C≡N group(s), for which “head-to-tail” disorder commonly occurs. The problem is exacerbated by the similar X-ray form factors for C

(24) Otwinowski, Z. *DENZO*; Department of Molecular Biophysics and Biochemistry, Yale University: New Haven, CT, 1993.

(25) Otwinowski, Z. *SCALEPACK*; Department of Molecular Biophysics and Biochemistry, Yale University: New Haven, CT, 1993.

(26) Altomare, A.; Cascarano, G.; Giacovazzo, C.; Guagliardi, A.; Burla, M. C.; Polidori, G.; Camelli, M. *J Appl. Crystallogr., Sect. A* **1994**, *27*, 435. SIR92.

(27) Watkin, D. J.; Prout, C. K.; Carruthers, J. R.; Betteridge, P. W.; Cooper, R. I. *CRYSTALS Issue 11*; Chemical Crystallography Laboratory, University of Oxford: Oxford, U.K., 2001.

Bending, Twisting, and Breaking CuCN Chains

and N and the almost identical M–C and M–N bond lengths. In two of the materials, Cs[Cu₃(CN)₃Cl] (**III**) and Cs[Cu₃(CN)₃Br] (**IV**), crystallographic symmetry means that C and N cannot be distinguished, and so in the final model, there is complete “head-to-tail” disorder in the C≡N group(s). In [Cu(H₂O)₄][Cu₄(CN)₄I₂] (**VI**), the C and N occupancies for the 4 positions corresponding to the two distinct C≡N groups refined to within 0.01 of 0.50/0.50 C/N and were therefore fixed at these values. A similar approach was adopted in the structural modeling of Cs₂[Cu₄(CN)₄I₂]·H₂O (**V**), which contains three distinct C≡N groups. One of these can theoretically order, by virtue of the space group symmetry (*C2/c*), while in the other two C≡N groups, the C and N atoms are indistinguishable by symmetry. The C/N occupancies for the first C≡N group refined to values close to 0.5/0.5, and these, together with the other sites whose occupations are fixed by symmetry, were set to 0.5/0.5. In [Cu(OH₂)₄][Cu₂(CN)I₂]₂ (**VII**), there is only one distinct C≡N group. The C occupancies of the two possible sites refined to values of 0.99(6) and 0.01(6), demonstrating that the C≡N group is ordered in this case, and these were set to 1.00 and 0.00 in the final refinement. The lower quality of the crystal of K₃[Cu₆(CN)₆I₃]·2H₂O (**II**) precluded the refinement of the C and N occupancies. Each position was therefore set to have occupancy of 0.5C and 0.5N.

FTIR Spectroscopy. The IR spectra of the unwashed polycrystalline products prepared at room temperature, compounds **I–V**, were measured in Nujol mulls using a Perkin-Elmer FTIR 1720-X spectrometer (Table 1).

Results and Discussion

Description of the Structures. The infinite $-(\text{CuCN})-$ chains, which are found in both LT- and HT-CuCN, are retained in all but one of the materials, namely [Cu(H₂O)₄][Cu₂(CN)I₂]₂ (**VII**). The structures of **I–VI** can be described in terms of bent and twisted chains linked by halogen bridges. These structures are rather different from that of [NBu₄][Cu(CN)X] (*X* = Br, I) characterized by Bowmaker et al.¹⁶ Although the latter materials also contain infinite halogenocyanocuprate chains, the halogen atoms are bonded to only one copper atom and do not act as bridging ligands. In the case of the simple AX–CuCN addition products, **I–V**, not only are the $-(\text{CuCN})-$ chains retained on their formation, but they are recovered when the alkali halide is washed out. The remaining materials, **VI** and **VII**, both contain [Cu(H₂O)₄]²⁺ and are mixed-valence compounds. Although [Cu^{II}(OH₂)₄][Cu^I₄(CN)₄I₂] (**VI**) also contains infinite $-(\text{CuCN})-$ chains, in the remaining material, [Cu(H₂O)₄][Cu₂(CN)I₂]₂ (**VII**), cleavage of the $-(\text{CuCN})-$ chains during synthesis leads to formation of discrete Cu–CN–Cu fragments.

Structures with Twisted $-(\text{CuCN})-$ Chains: **III and **IV**.** Cs[Cu₃(CN)₃Cl] (**III**) and Cs[Cu₃(CN)₃Br] (**IV**) are isostructural (Table 4) and consist of helical $-(\text{CuCN})-$ chains running parallel to the *c*-axis, linked through halogen atoms to form two interpenetrating negatively charged frameworks of formula [Cu₃(CN)₃X][−], which are charge balanced by Cs cations (Figure 1a). The coordination around both copper and halogen atoms is trigonal planar with Cu–C/N and Cu–Cl lengths of 1.883(4) and 2.4673(11) Å in **III** and Cu–C/N and Cu–Br lengths of 1.853(8) and 2.599(2) Å in **IV**. The binding of the halogen atoms in the $-(\text{CuCN})-$ chains has caused the C/N–Cu–C/N bond

Table 4. Selected Bond Lengths (Å) and Angles (deg) for Cs[Cu₃(CN)₃Cl] (**III**) and Cs[Cu₃(CN)₃Br] (**IV**)^a

Cs[Cu ₃ (CN) ₃ Cl] (III)		Cs[Cu ₃ (CN) ₃ Br] (IV)	
Cu(1)–Cl(1)	2.4673(11)	Cu(1)–Br(1)	2.599(2)
Cu(1)–Z(1)	1.883(4)	Cu(1)–Z(1)	1.853(8)
Cu(1)–Z(1)′	1.883(4)	Cu(1)–Z(1)	1.853(8)
Z(1)–Z(1)′	1.149(9)	Z(1)–Z(1)′	1.203(17)
Cl(1)–Cu(1)–Z(1)	108.12(15)	Br(1)–Cu(1)–Z(1)	106.5(3)
Cl(1)–Cu(1)–Z(1)′	108.12(15)	Br(1)–Cu(1)–Z(1)′	106.5(3)
Z(1)–Cu(1)–Z(1)′	143.8(3)	Z(1)–Cu(1)–Z(1)′	146.9(6)
Cu(1)–Cl(1)–Cu(1)′	120	Cu(1)–Br(1)–Cu(1)′	120
Cu(1)–Cl(1)–Cu(1)′′	120	Cu(1)–Br(1)–Cu(1)′′	120
Cu(1)′–Cl(1)–Cu(1)′′	120	Cu(1)′–Br(1)–Cu(1)′′	120
Cu(1)–Z(1)–Z(1)′	176.8(4)	Cu(1)–Z(1)–Z(1)′	178.4(3)

^a Z = either C or N of a disordered cyanide group.

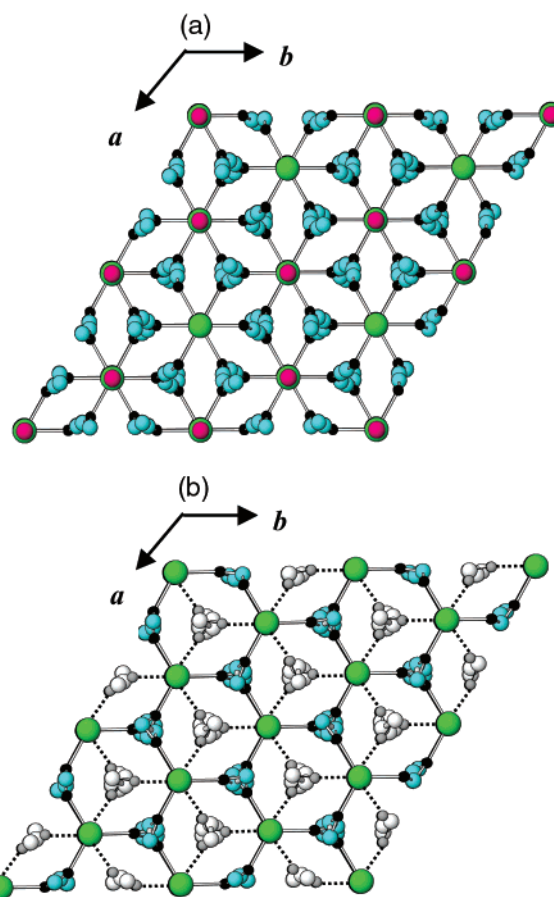


Figure 1. (a) View of Cs[Cu₃(CN)₃Br] (**IV**) showing helical $-(\text{CuCN})-$ chains running parallel to the *c*-axis linked together by trigonally coordinated bromine atoms. Cs⁺ ions lie in columns running down the *c*-axis between adjacent bromine atoms. Cs[Cu₃(CN)₃Cl] (**III**) is isostructural. (b) View showing the two separate interpenetrating [Cu₃(CN)₃Br][−] sublattices in **IV**. One sublattice is shown in color and linked by full bonds, and the other is shown in grayscale and linked by dashed lines to represent bonds. Key: Cu, black spheres; C/N, cyan; Br, green; Cs, magenta. Drawing package: ATOMS.²⁸

angles to close from $\sim 180^\circ$, as found in LT- and HT-CuCN,^{20,21} to 143.8(3)° and 146.9(6)° for **III** and **IV**, respectively. The individual $-(\text{CuCN})-$ chains form helices which repeat every third CuCN unit. Each $-(\text{CuCN})-$ chain is bonded to six other chains of the same handedness via the halogen atoms to generate a network (Figure 1b). A second network of opposite handedness is generated in the

Table 5. Selected Bond Lengths (Å) and Angles (deg) for $K[Cu_2(CN)_2Br] \cdot H_2O$ (**I**)^a

Cu(1)–Br(1)	2.6864(8)	Z(1)–Cu(1)–Z(2)	146.21(19)
Cu(1)–Br(1)′	2.7229(8)		
Cu(1)–Z(1)	1.890(4)	Cu(1)–Br(1)–Cu(1)′	173.12(2)
Cu(1)–Z(2)	1.889(4)	Cu(1)–Br(1)–Cu(1)′′	90.75(3)
Z(1)–Z(2)	1.144(6)	Cu(1)–Br(1)–Cu(1)′′′	89.618(19)
Br(1)–Cu(1)–Br(1)′	88.961(19)	Cu(1)–Z(1)–Z(2)	173.8(4)
Br(1)–Cu(1)–Z(1)	101.78(12)	Cu(1)–Z(2)–Z(1)	172.2(4)
Br(1)′–Cu(1)–Z(1)	103.98(12)		
Br(1)–Cu(1)–Z(2)	103.26(12)		
Br(1)′–Cu(1)–Z(2)	98.81(13)		

^a Z = either C or N of a disordered cyanide group.

same way. The two networks interpenetrate so that each $-(CuCN)-$ chain has as its nearest neighbors three $-(CuCN)-$ chains from the other network and the halogen atoms from both networks lie on top of each other to form columns running parallel to *c*. Cesium ions lie equidistant between pairs of halogen atoms within these columns (bond lengths: Cs–Cl, 3.462(1) Å in **III**, and Cs–Br, 3.496(1) Å in **IV**) and have 12 C/N neighbors with Cs–C/N distances in the range 3.49–3.51 Å (**III**) and 3.53–3.58 Å (**IV**).

Structures with Bent $-(CuCN)-$ Chains: **I, **II**, **V**, and **VI**.** Although $K[Cu_2(CN)_2Br] \cdot H_2O$ (**I**), $K_3[Cu_6(CN)_6I_3] \cdot 2H_2O$ (**II**), $Cs_2[Cu_4(CN)_4I_2] \cdot H_2O$ (**V**), and $[Cu(H_2O)_4][Cu_4(CN)_4I_2] \cdot H_2O$ (**VI**) all contain $-(CuCN)-$ chains linked by halogen atoms to form 3-D halogenocyanocuprate frameworks with the empirical formula $[Cu_2(CN)_2X]^-$ ($X = Br, I$), they adopt rather different structures. These frameworks are more open than the ones described above for **III** and **IV** as they have room to include hydrated cations in interchain cavities.

We have previously reported the structure of $K[Cu_2(CN)_2Br] \cdot H_2O$ (**I**) determined at 150 K.²⁰ This material is closely related to the new materials reported here. We therefore include a description of this structure, together with the values for important bond lengths determined at room temperature, to facilitate discussion (Table 5). In $K[Cu_2(CN)_2Br] \cdot H_2O$ (**I**), adjacent $-(CuCN)-$ chains are linked together via bromine atoms to generate a three-dimensional framework of formula $[Cu_2(CN)_2Br]^-$ containing a 2-D pore network in which K^+ and H_2O reside (Figure 2). Each Cu atom is attached to two cyanide groups and two bromine atoms to produce a very distorted tetrahedral coordination with Cu–C/N lengths of 1.889(4) and 1.890(4) Å, Cu–Br lengths of 2.686(1) and 2.723(1) Å, and a C/N–Cu–C/N bond angle of 146.21(19)°. The bromine atom adopts square-planar coordination with respect to copper and also interacts with the extraframework potassium ion (K–Br, 3.290(2) Å). The potassium ion, as well as being coordinated to bromine, has two water molecules (K–O distances of 2.798(6) and 2.926(6) Å) and 8 C/N atoms within its coordination sphere (K–C/N distances in the range 3.31–3.42 Å).

$K_3[Cu_6(CN)_6I_3] \cdot 2H_2O$ (**II**) also contains bent $-(CuCN)-$ chains linked through halogen atoms to form an open framework accommodating K^+ and H_2O in a 2-D pore network (Figure 3a). However, this structure is more complicated than those of **I**, **III**, and **IV**, because it contains three distinct types of copper atoms within each $-(CuCN)-$ chain (Table 6). One of the copper atoms, Cu(2), has an

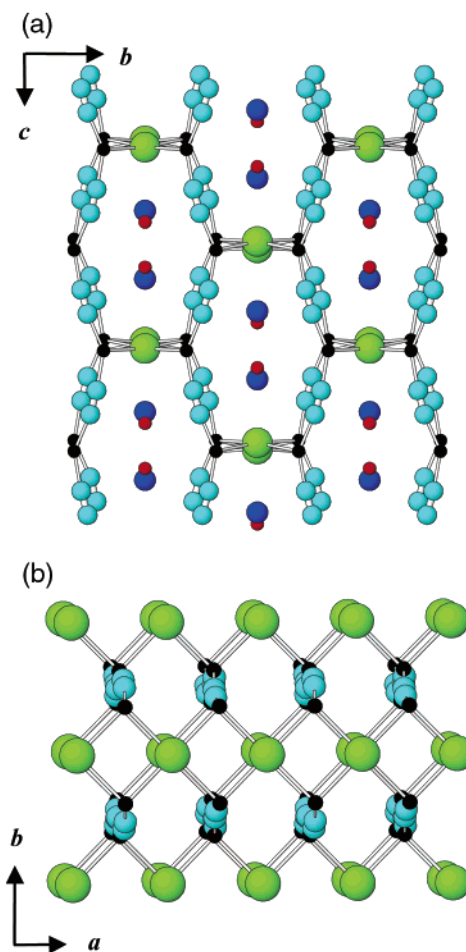


Figure 2. (a) View along the *a*-axis of $K[Cu_2(CN)_2Br] \cdot H_2O$ (**I**) showing channels formed by linking of $-(CuCN)-$ chains by bromine atoms to generate pores in which hydrated K^+ ions reside. (b) View along the *c*-axis of the $[Cu_2(CN)_2Br]^-$ framework showing linking of adjacent $-(CuCN)-$ chains by bromine atoms which have square-planar coordination. Key: Cu, black spheres; C/N, cyan; Br, green; K, blue; O, red. Hydrogen atoms have been omitted.

environment similar to those of copper in LT- and HT-CuCN in that it is only coordinated to cyanide groups and has an approximately linear C/N–Cu(2)–C/N geometry. The remaining copper atoms, Cu(1) and Cu(3), are coordinated to two iodine atoms as well as two cyanide groups in a very distorted tetrahedral geometry (bond lengths: Cu(1)–I(1), 2.747(3) and 2.993(3) Å, Cu(3)–I(1), 2.867(4) Å, and Cu(3)–I(2), 2.859(4) Å). The C/N–Cu(1)–C/N and C/N–Cu(3)–C/N bond angles, of 133.9(9) and 129.1(8)°, respectively, are more acute than those found in structures **I**, **III**, and **IV**, reflecting the strong interaction of Cu(1) and Cu(3) with the iodine atoms. Of the two distinct iodine atoms, one, I(1), is coordinated to three copper neighbors in rather irregular geometry while the other, I(2), is two-coordinate (Figure 3b). The iodine atoms link the $-(CuCN)-$ chains: I(2) bridges two Cu(3) atoms in different chains and I(1) bridges three different chains bonding to two Cu(1) and one Cu(3) atom to give a framework of empirical formula $[Cu_2(CN)_2I]^-$. The potassium ions and water molecules lie in channels running parallel to the *a*-axis. Both K(1) and K(2) are coordinated by iodine, water, and C/N (bond

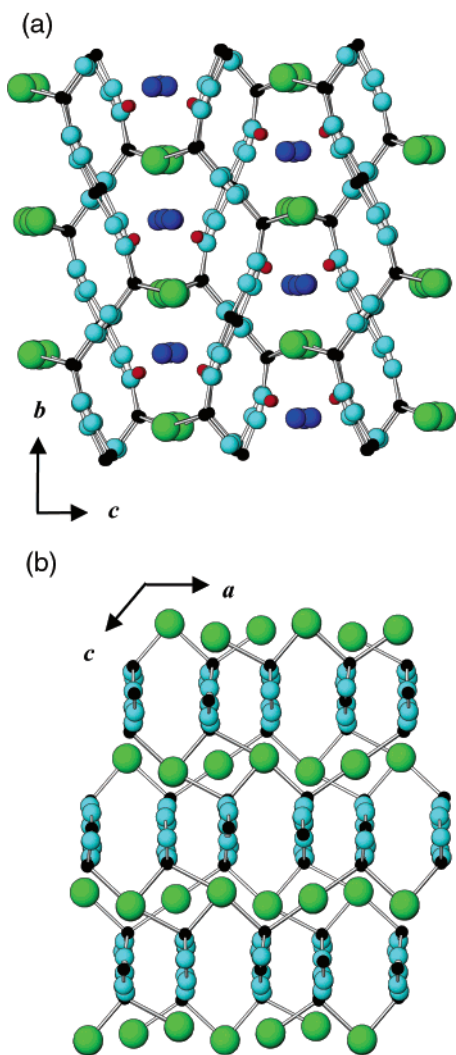


Figure 3. (a) View along the *a*-axis of $K_3[Cu_6(CN)_6I_3] \cdot 2H_2O$ (**II**) showing channels formed by linking of $-(CuCN)-$ chains by iodine atoms to generate pores in which hydrated K^+ ions reside. (b) View along the *b*-axis of the $[Cu_6(CN)_6I_3]^{3-}$ framework showing linking of adjacent $-(CuCN)-$ chains by iodine atoms which are two- and three-coordinate. Key: Cu, black spheres; C/N, cyan; I, green; K, blue; O, red. Hydrogen atoms have been omitted.

lengths: $K(1)-I$, 3.631(8), $2 \times 3.636(6)$ Å, $K(1)-O$, $2 \times 2.721(19)$ Å with 6 C/N atoms within the range 3.43–3.56 Å; $K(2)-I$, 3.615(5), 3.702(18), and 3.732(5) Å, $K(2)-O$, 2.730(18) Å with 8 C/N atoms within the range 3.12–3.37 Å).

$Cs_2[Cu_4(CN)_4I_2] \cdot H_2O$ (**V**) has a three-dimensional framework of formula $[Cu_4(CN)_4I_2]^{2-}$ with a 3-D pore system containing Cs^+ and water molecules (Figure 4). The framework is constructed from infinite $-(CuCN)-$ chains linked by three-coordinate iodine atoms. The $-(CuCN)-$ chains contain two types of copper atoms, Cu(1) and Cu(2), which occur in the sequence Cu(1)–Cu(1)–Cu(2)–Cu(2) along each chain (Table 7). Additional bonding of iodine atoms, two to Cu(1) (bond lengths: Cu(1)–I(1), 2.6938(18) and 2.7706(19) Å), and one to Cu(2) (Cu(2)–I(1), 2.810(2) Å), gives rise to tetrahedral and trigonal geometries, respectively, around copper. The C/N–Cu(1)–C/N bond angle of $119.9(4)^\circ$ reflects the fact that Cu(1) is very strongly bound to two

Table 6. Selected Bond Lengths (Å) and Angles (deg) for $K_3[Cu_6(CN)_6I_3] \cdot 2H_2O$ (**II**)^a

Cu(1)–I(1)	2.747(3)	Z(2)–Cu(2)–Z(3)	175.4(9)
Cu(1)–I(1')	2.993(3)	I(1)–Cu(3)–I(2)	99.66(9)
Cu(1)–Z(1)	1.859(19)	I(1)–Cu(3)–Z(4)	105.4(6)
Cu(1)–Z(5)	1.925(17)	I(2)–Cu(3)–Z(4)	111.0(6)
Cu(2)–Z(2)	1.842(18)	I(1)–Cu(3)–Z(6)	101.8(5)
Cu(2)–Z(3)	1.845(19)	I(2)–Cu(3)–Z(6)	105.7(5)
Cu(3)–I(1)	2.867(4)	Z(4)–Cu(3)–Z(6)	129.1(8)
Cu(3)–I(2)	2.859(4)		
Cu(3)–Z(4)	1.926(19)	Cu(1)–I(1)–Cu(1')	75.27(9)
Cu(3)–Z(6)	1.926(19)	Cu(1)–I(1)–Cu(3)	85.22(11)
Z(1)–Z(2)	1.22(3)	Cu(1)'–I(1)–Cu(3)	153.03(9)
Z(3)–Z(4)	1.15(3)	Cu(3)–I(2)–Cu(3)'	159.72(13)
Z(5)–Z(6)	1.13(2)		
		Cu(1)–Z(1)–Z(2)	169.9(18)
I(1)–Cu(1)–I(1')	99.52(9)	Cu(2)–Z(2)–Z(1)	170.3(17)
I(1)–Cu(1)–Z(1)	109.6(6)	Cu(2)–Z(3)–Z(4)	174.3(19)
I(1)'–Cu(1)–Z(1)	103.8(7)	Cu(3)–Z(4)–Z(3)	167.6(18)
I(1)–Cu(1)–Z(5)	106.5(5)	Cu(1)–Z(5)–Z(6)	177.8(18)
I(1)'–Cu(1)–Z(5)	97.5(5)	Cu(3)–Z(6)–Z(5)	174.4(15)
Z(1)–Cu(1)–Z(5)	133.9(9)		

^a Z = either C or N of a disordered cyanide group.

iodine atoms. The bond angle for C/N–Cu(2)–C/N of $137.0(5)^\circ$ is more obtuse because Cu(2) is only bound to one iodine atom. However, this angle is slightly smaller than the corresponding ones observed in **III** and **IV**, which also contain copper atoms connected to three-coordinate halogen atoms. This angle closing probably arises because there is an additional interaction between Cu(2) and a cyanide group in a neighboring chain (Cu(2)···C/N(3), 2.371(9) Å) (Figure 4b). A further consequence of this interchain interaction is that the Cu(1)–C/N(3)–C/N(3)' bond angle within the $-(CuCN)-$ chain is $157.4(7)^\circ$, in contrast to the Cu–C/N–C/N' angles which are close to 180° in all the compounds discussed so far. The bonding of the C/N(3)–C/N(3)' cyanide group can be viewed as intermediate between the μ_2 -coordination shown by cyanide groups elsewhere in this paper and μ_4 -coordination found by Guo and Mak in the silver cyanide–silver fluoride addition compound, $3AgCN \cdot 2AgF \cdot 3H_2O$.²⁹ The cesium ion is coordinated to two iodine atoms and one water molecule (Cs–I distances of 3.866(1) and 3.953(1) Å and Cs–O distance of 3.062(11) Å) and 10 C/N atoms within its coordination sphere with Cs–C/N distances in the range 3.47–3.98 Å.

The framework of $[Cu(H_2O)_4][Cu_4(CN)_4I_2]$ (**VI**) has the same stoichiometry as that of **V**, but in this case, the negative charge is balanced by the complex cation $[Cu^II(H_2O)_4]^{2+}$ to generate a mixed-valence compound (Figure 5). Although the geometries around the two distinct Cu atoms are similar to those in **V**, consisting of very distorted tetrahedral Cu(1) and trigonal Cu(2) geometries (bond lengths: Cu(1)–I(1), 2.7240(13) and 2.9392(17) Å; Cu(2)–I(1), 2.8341(15) Å), the Cu(1)–Cu(2)–Cu(1)–Cu(2) arrangement of the copper atoms along the infinite $-(CuCN)-$ chains produces a different framework (Table 8). Again, the C/N–Cu(1)–C/N bond angle of $124.6(3)^\circ$ reflects the strength of the two Cu(1)–iodine interactions while the C/N–Cu(2)–C/N bond angle of $142.5(3)^\circ$ is similar to those observed in **III** and

(28) Dowty, E. *ATOMS*, v. 5.1; Shape Software: Kingsport, TN, 2000.

(29) Guo, G. C.; Mak, T. C. W. *Angew. Chem., Int. Ed.* **1998**, *37*, 3183.

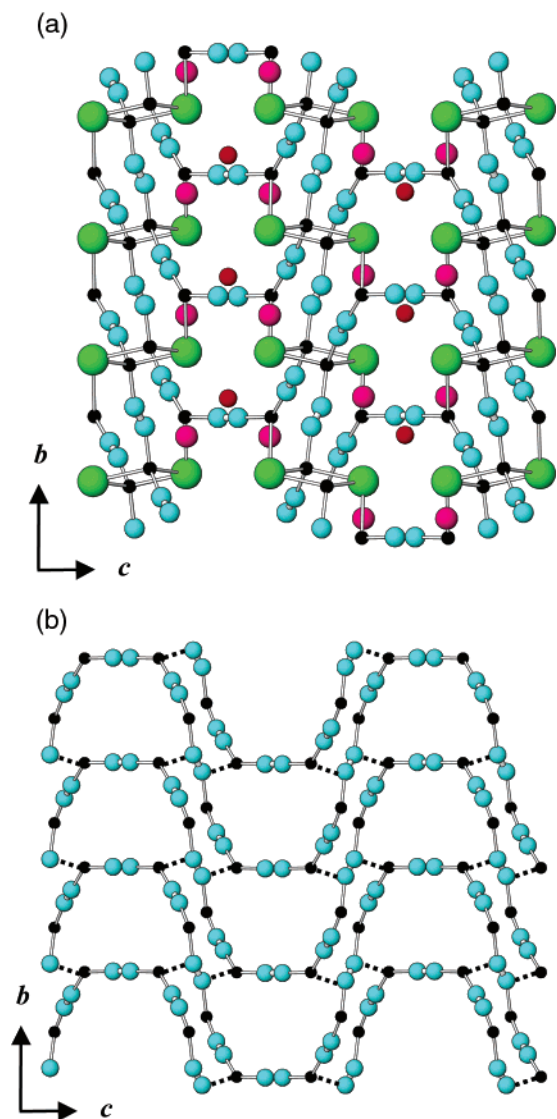


Figure 4. (a) View of $\text{Cs}_2[\text{Cu}_4(\text{CN})_4\text{I}_2]\cdot\text{H}_2\text{O}$ (V) along the a -axis showing the linking of $-(\text{CuCN})-$ chains by three-coordinate iodine atoms to generate channels. Hydrated Cs^+ ions reside in the pore walls. (b) View along the a -axis of the wavelike $-(\text{CuCN})-$ chains in V with the weak interchain $\text{Cu}\cdots\text{C/N}$ bonds shown as dashed lines. Key: Cu, black spheres; C/N, cyan; I, green; Cs, magenta; O, red. Hydrogen atoms have been omitted.

IV. The iodine atoms link three different $-(\text{CuCN})-$ chains connecting to two $\text{Cu}(1)$ atoms and one $\text{Cu}(2)$ atom to generate a three-dimensional framework containing a 3-D pore system in which the square-planar $[\text{Cu}(3)(\text{H}_2\text{O})_4]^{2+}$ cations reside. The cations are held in position by weak interactions to two framework iodine atoms ($\text{Cu}(3)-\text{I}(1)$, $2 \times 3.2228(5)$ Å), which complete the tetragonally distorted octahedral coordination. Presumably, weak hydrogen bonding between $\text{O}(1)\text{H}_2$ groups and framework C/N atoms prevents rotation of the cation about the $\text{I}-\text{Cu}(3)-\text{I}'$ axis.

Structure Containing a Single Cu–CN–Cu Link of the $-(\text{CuCN})-$ Chain: VII. $[\text{Cu}(\text{OH}_2)_4][\text{Cu}_2(\text{CN})_2\text{I}_2]$ (VII), like VI, is also a mixed-valence compound containing $[\text{Cu}^{\text{II}}(\text{H}_2\text{O})_4]^{2+}$ cations (Figure 6). The structure of this compound differs from all those described above in that the anionic framework, of formula $[\text{Cu}_2(\text{CN})_2\text{I}_2]^-$, is layered rather than

Table 7. Selected Bond Lengths (Å) and Angles (deg) for $\text{Cs}_2[\text{Cu}_4(\text{CN})_4\text{I}_2]\cdot\text{H}_2\text{O}$ (V)^a

$\text{Cu}(1)-\text{I}(1)$	2.6983(18)	$\text{I}(1)-\text{Cu}(2)-\text{Z}(1)$	106.2(3)
$\text{Cu}(1)-\text{I}(1')$	2.7706(19)	$\text{I}(1)-\text{Cu}(2)-\text{Z}(4)$	103.0(3)
$\text{Cu}(1)-\text{Z}(2)$	1.94(1)	$\text{Z}(1)-\text{Cu}(2)-\text{Z}(4)$	137.0(5)
$\text{Cu}(1)-\text{Z}(3)$	1.977(6)		
$\text{Cu}(2)-\text{I}(1)$	2.810(2)	$\text{Cu}(1)-\text{I}(1)-\text{Cu}(1')$	72.56(6)
$\text{Cu}(2)-\text{Z}(1)$	1.898(11)	$\text{Cu}(1)-\text{I}(1)-\text{Cu}(2)$	65.46(5)
$\text{Cu}(2)-\text{Z}(4)$	1.91(1)	$\text{Cu}(1')-\text{I}(1)-\text{Cu}(2)$	107.49(5)
$\text{Z}(1)-\text{Z}(2)$	1.165(15)	$\text{Cu}(2)-\text{Z}(1)-\text{Z}(2)$	176.7(9)
$\text{Z}(3)-\text{Z}(3')$	1.124(9)		
$\text{Z}(4)-\text{Z}(4')$	1.152(19)	$\text{Cu}(1)-\text{Z}(2)-\text{Z}(1)$	174.4(10)
		$\text{Cu}(1)-\text{Z}(3)-\text{Z}(3')$	157.5(12)
$\text{I}(1)-\text{Cu}(1)-\text{I}(1')$	107.44(6)	$\text{Cu}(2)-\text{Z}(4)-\text{Z}(4')$	178.9(3)
$\text{I}(1)-\text{Cu}(1)-\text{Z}(2)$	109.2(3)		
$\text{I}(1')-\text{Cu}(1)-\text{Z}(2)$	108.8(3)		
$\text{I}(1)-\text{Cu}(1)-\text{Z}(3)$	110.5(3)		
$\text{I}(1')-\text{Cu}(1)-\text{Z}(3)$	100.0(3)		
$\text{Z}(2)-\text{Cu}(1)-\text{Z}(3)$	119.9(4)		

^a Z = either C or N of a disordered cyanide group.

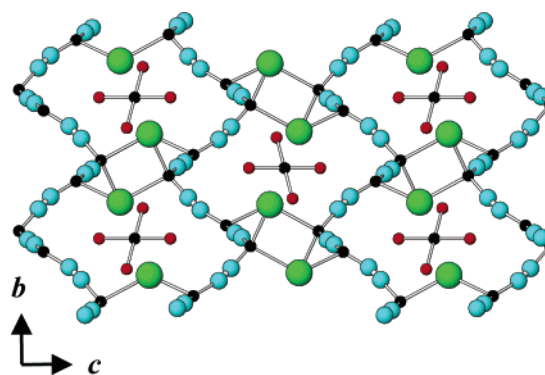


Figure 5. View along the a -axis of $[\text{Cu}(\text{H}_2\text{O})_4][\text{Cu}_4(\text{CN})_4\text{I}_2]$ (VI) showing wavelike $-(\text{Cu}-\text{CN})-$ chains linked through three-coordinate iodine atoms to generate channels. Square-planar $[\text{Cu}(\text{H}_2\text{O})_4]^{2+}$ cations reside in the channels between pairs of iodine atoms. Key: Cu, black spheres; C/N, cyan; I, green; O, red. Hydrogen atoms have been omitted.

Table 8. Selected Bond Lengths (Å) and Angles (deg) for $[\text{Cu}(\text{H}_2\text{O})_4][\text{Cu}_4(\text{CN})_4\text{I}_2]$ (VI)^a

$\text{Cu}(1)-\text{I}(1)$	2.7240(13)	$\text{I}(1)-\text{Cu}(2)-\text{Z}(2)$	105.5(3)
$\text{Cu}(1)-\text{I}(1')$	2.9392(17)	$\text{I}(1)-\text{Cu}(2)-\text{Z}(4)$	101.1(2)
$\text{Cu}(1)-\text{Z}(1)$	1.942(8)	$\text{Z}(2)-\text{Cu}(2)-\text{Z}(4)$	142.5(3)
$\text{Cu}(1)-\text{Z}(3)$	1.92(1)		
$\text{Cu}(2)-\text{I}(1)$	2.8341(15)	$\text{O}(1)-\text{Cu}(3)-\text{O}(1')$	180
$\text{Cu}(2)-\text{Z}(2)$	1.894(9)	$\text{O}(1)-\text{Cu}(3)-\text{O}(2) \times 2$	88.9(4)
$\text{Cu}(2)-\text{Z}(4)$	1.90(1)	$\text{O}(1')-\text{Cu}(3)-\text{O}(2) \times 2$	91.1(4)
		$\text{O}(2)-\text{Cu}(3)-\text{O}(2')$	180
$\text{Cu}(3)-\text{O}(1)$	2.003(7)		
$\text{Cu}(3)-\text{O}(2)$	2.044(8)	$\text{Cu}(1)-\text{I}(1)-\text{Cu}(1')$	86.02(4)
		$\text{Cu}(1)-\text{I}(1)-\text{Cu}(2)$	64.01(4)
$\text{Z}(1)-\text{Z}(2)$	1.131(11)	$\text{Cu}(1')-\text{I}(1)-\text{Cu}(2)$	123.09(4)
$\text{Z}(3)-\text{Z}(4)$	1.136(3)	$\text{Cu}(1)-\text{I}(1)-\text{Cu}(3)$	156.94(3)
		$\text{Cu}(1')-\text{I}(1)-\text{Cu}(3)$	95.47(3)
$\text{I}(1)-\text{Cu}(1)-\text{I}(1')$	93.98(4)	$\text{Cu}(2)-\text{I}(1)-\text{Cu}(3)$	96.67(3)
$\text{I}(1)-\text{Cu}(1)-\text{Z}(1)$	108.8(2)		
$\text{I}(1')-\text{Cu}(1)-\text{Z}(1)$	107.4(3)	$\text{Cu}(1)-\text{Z}(1)-\text{Z}(2)$	175.1(8)
$\text{I}(1)-\text{Cu}(1)-\text{Z}(3)$	115.5(3)	$\text{Cu}(2)-\text{Z}(2)-\text{Z}(1)$	175.9(8)
$\text{I}(1')-\text{Cu}(1)-\text{Z}(3)$	101.3(2)	$\text{Cu}(1)-\text{Z}(3)-\text{Z}(4)$	177.6(7)
$\text{Z}(1)-\text{Cu}(1)-\text{Z}(3)$	124.6(3)	$\text{Cu}(2)-\text{Z}(4)-\text{Z}(3)$	167.4(7)

^a Z = either C or N of a disordered cyanide group.

three-dimensional, the cyanide group is fully ordered, i.e., C(1) and N(1) are distinguishable, and the $-(\text{CuCN})-$ chains, persistent in all the other materials, have been broken leaving only a single $\text{Cu}(2)-\text{CN}-\text{Cu}(1)$ link as the copper–cyanide building unit. In this unit, $\text{Cu}(1)$ is also coordinated

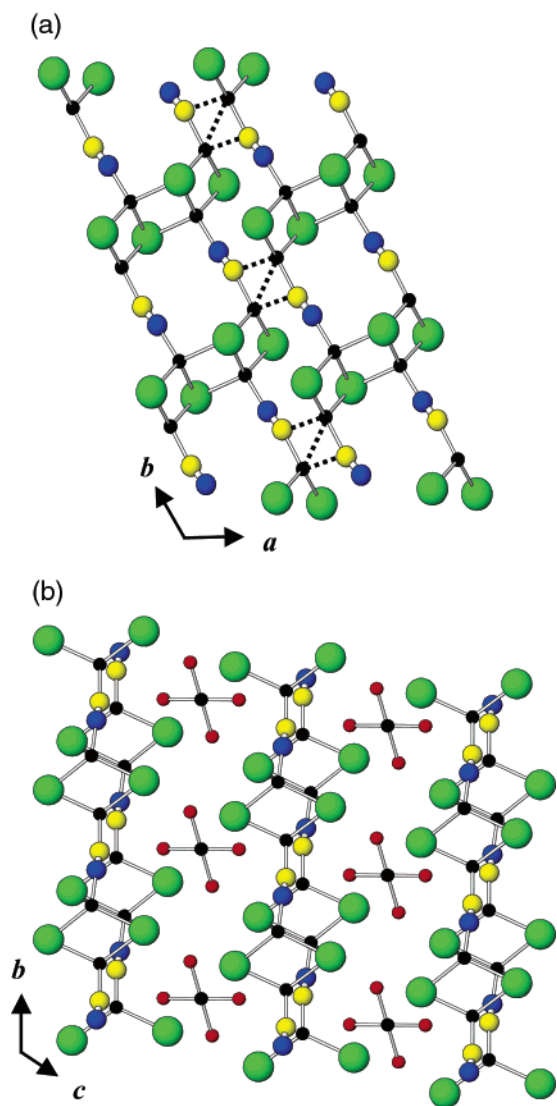


Figure 6. (a) Linking of the $[\text{Cu}_2(\text{CN})_2]^{2-}$ chains in **VII** into layers by secondary $\text{Cu}\cdots\text{C}$ and $\text{Cu}\cdots\text{Cu}$ interactions indicated by dashed lines. (b) View along the a -axis of $[\text{Cu}(\text{OH}_2)_4][\text{Cu}_2(\text{CN})_2]_2$ (**VII**) showing the arrangement of the $[\text{Cu}_2(\text{CN})_2]^{2-}$ layers and the square-planar $[\text{Cu}(\text{H}_2\text{O})_4]^{2+}$ cations between them. Key: Cu, black spheres; C, yellow; N, blue; I, green; O, red. Hydrogen atoms have been omitted.

to three iodine atoms (with $\text{Cu}(1)\text{--I}$ distances of 2.6750(8), 2.6825(9), and 2.714(1) Å) and $\text{Cu}(2)$ to two iodine atoms (with $\text{Cu}(2)\text{--I}$ distances of 2.6212(7) and 2.6527(8) Å) (Table 9). The iodine atoms serve to link the $\text{Cu}\text{--CN}\text{--Cu}$ units together to form $[\text{Cu}_4(\text{CN})_2\text{I}_4]^{2-}$ chains running parallel to the b -axis. A number of additional interactions involving the $\text{Cu}(2)$ atoms in the $[\text{Cu}_4(\text{CN})_2\text{I}_4]^{2-}$ chains link them into layers in the ab -plane (Figure 6a). The $\text{Cu}(2)\cdots\text{Cu}(2')$ distance between adjacent chains is rather short (at 2.518(1) Å) implying some significant bonding contribution. In addition, there is bonding between $\text{Cu}(2)$ in one $[\text{Cu}_4(\text{CN})_2\text{I}_4]^{2-}$ chain and the carbon atom of a cyanide group in a neighboring chain ($\text{Cu}(2)\cdots\text{C}(1')$, 2.330(6) Å), a feature observed previously in **V**. A further consequence of both these interactions involving $\text{Cu}(2)$ is that the $\text{Cu}(2)\text{--C}(1)\text{--N}(1)$ bond angle within the $\text{Cu}(2)\text{--CN}\text{--Cu}(1)$ link is $166.3(5)^\circ$.

Table 9. Selected Bond Lengths (Å) and Angles (deg) for $[\text{Cu}(\text{H}_2\text{O})_4][\text{Cu}_2(\text{CN})_2]_2$ (**VII**)

$\text{Cu}(1)\text{--I}(1)$	2.6825(9)	$\text{I}(1)\text{--Cu}(2)\text{--I}(2)$	117.89(3)
$\text{Cu}(1)\text{--I}(2)$	2.6750(8)	$\text{I}(1)\text{--Cu}(2)\text{--C}(1)$	115.64(14)
$\text{Cu}(1)\text{--I}(2)'$	2.714(1)	$\text{I}(2)\text{--Cu}(2)\text{--C}(1)$	112.78(14)
$\text{Cu}(1)\text{--N}(1)$	1.969(4)	$\text{O}(1)\text{--Cu}(3)\text{--O}(1)'$	180
$\text{Cu}(2)\text{--I}(1)$	2.6212(7)	$\text{O}(1)\text{--Cu}(3)\text{--O}(2) \times 2$	90.8(2)
$\text{Cu}(2)\text{--I}(2)$	2.6527(8)	$\text{O}(1)'\text{--Cu}(3)\text{--O}(2) \times 2$	89.2(2)
$\text{Cu}(2)\text{--C}(1)$	1.975(5)	$\text{O}(2)\text{--Cu}(3)\text{--O}(2)'$	180
$\text{Cu}(3)\text{--O}(1) \times 2$	2.012(5)	$\text{Cu}(1)\text{--I}(1)\text{--Cu}(2)$	63.66(2)
$\text{Cu}(3)\text{--O}(2) \times 2$	2.026(5)	$\text{Cu}(1)\text{--I}(2)\text{--Cu}(1)'$	70.81(3)
$\text{C}(1)\text{--N}(1)$	1.118(7)	$\text{Cu}(1)\text{--I}(2)\text{--Cu}(2)$	63.35(2)
$\text{I}(1)\text{--Cu}(1)\text{--I}(2)$	114.99(3)	$\text{Cu}(1)'\text{--I}(2)\text{--Cu}(2)$	99.07(3)
$\text{I}(1)\text{--Cu}(1)\text{--I}(2)'$	101.85(3)	$\text{Cu}(1)\text{--N}(1)\text{--C}(1)$	173.0(5)
$\text{I}(2)\text{--Cu}(1)\text{--I}(2)'$	109.19(3)	$\text{Cu}(2)\text{--C}(1)\text{--Cu}(2)'$	71.04(17)
$\text{I}(1)\text{--Cu}(1)\text{--N}(1)$	114.16(13)	$\text{Cu}(2)\text{--C}(1)\text{--N}(1)$	166.3(5)
$\text{I}(2)\text{--Cu}(1)\text{--N}(1)$	108.09(13)		
$\text{I}(2)'\text{--Cu}(1)\text{--N}(1)$	108.15(13)		

In compounds **I–VI**, the halogen atoms are responsible for linking adjacent $\text{--}(\text{CuCN})\text{--}$ chains into three-dimensional frameworks. Here in **VII**, the major bonding role of the iodine atoms is in the formation of the $[\text{Cu}_4(\text{CN})_2\text{I}_4]^{2-}$ chains, which in turn form a two-dimensional framework. The coordination of $\text{I}(2)$ is satisfied by bonding to three Cu atoms within a $[\text{Cu}_4(\text{CN})_2\text{I}_4]^{2-}$ chain. In the case of $\text{I}(1)$, which is coordinated to two Cu atoms within the $[\text{Cu}_4(\text{CN})_2\text{I}_4]^{2-}$ chain, there are additional weak interactions to the square-planar $[\text{Cu}(3)(\text{H}_2\text{O})_4]^{2+}$ cations lying between the layers ($\text{Cu}(3)\text{--I}(1)$, $2 \times 3.343(1)$ Å) completing the tetragonally distorted octahedral coordination around Cu^{2+} (Figure 6c). Weak hydrogen bonding between the OH_2 groups of the complex and framework N atoms further hold the complex ion in position.

Infrared Spectroscopy: The $\nu(\text{C}\equiv\text{N})$ Region. It is not easy to account for the $\text{C}\equiv\text{N}$ stretching frequencies observed in the IR spectra of compounds **I–V**, particularly in those cases where there is more than one type of cyanide group present in the structure (Table 1). However, it is possible to make some general comments and relate some of the spectroscopic observations to the structures. At the simplest level, compounds **III** and **IV**, which are isostructural and contain one crystallographically distinct --CN group, have similar $\nu(\text{C}\equiv\text{N})$ frequencies, with the more intense of the two bands occurring at a lower wavenumber in each case. Furthermore, compound **I**, which also contains one crystallographically distinct --CN group and has $\text{--}(\text{CuCN})\text{--}$ chains bent to a similar degree as those in **III** and **IV**, shows a similar IR spectrum in this region. All three spectra contain the same number of peaks in the $\text{C}\equiv\text{N}$ stretching region as LT- and HT-CuCN, and their wavenumbers are similar (LT-CuCN, $\nu(\text{C}\equiv\text{N})$ 2166(vs) and 2118(m) cm^{-1} ; HT-CuCN, $\nu(\text{C}\equiv\text{N})$ 2167(vs) and 2120(m, sh) cm^{-1}).²⁰ However, the relative intensities of the two bands are reversed, reflecting the fact that the $\text{--}(\text{CuCN})\text{--}$ chains are significantly bent around copper in the addition products.

General Discussion

Reactions. Six of the seven compounds described here, **I–VI**, retain the covalently bonded $\text{--}(\text{CuCN})\text{--}$ chains

present in LT-CuCN, from which they were prepared, whereas in the seventh, **VII**, the chains are broken into individual Cu–CN–Cu links. Compounds **VI** and **VII** can only be prepared under forcing hydrothermal conditions which cause some of the Cu^I present to be oxidized to Cu^{II} and cause the destruction of at least some of the –(CuCN)– chains. In contrast, **I–V** are prepared rapidly at room temperature, and it is tempting to conclude that they are formed topochemically because the formation reactions proceed without any apparent dissolution of the solid CuCN and the topology of the –(CuCN)– chains is the same in the starting material and the products. The formation of cyanocuprate or halogenocyanocuprate species in solution followed by precipitation reactions to form the AX–CuCN addition compounds cannot at this stage be ruled out. However, it is more difficult to envisage copper-containing solution species being involved in the reverse reactions, that re-form solid CuCN on washing, when the alkali halide is no longer present in vast excess. This points to the reactions being topochemical in nature. It is notable that NaCl, NaBr, NaI, and KCl do not form addition compounds with CuCN under the conditions used here. Presumably, this is because the free energies of hydration of the alkali-metal and halide ions outweigh the corresponding energies for any possible addition compounds. These energies depend on both ionic sizes of the cations and anions and the relative hardnesses of the halides.

Structures. In **I–VI**, the –(CuCN)– chains become bent and twisted as a consequence of the attachment of halogen atoms. This contrasts with the situation in the two polymorphs of CuCN. In HT-CuCN, the N/C–Cu–C/N and Cu–C/N–N/C bond angles are both fixed by symmetry at 180°, and in LT-CuCN, they deviate only slightly from linearity (N/C–Cu–C/N angles lie in the range 176.7(3)–179.0(5)° and Cu–C/N–N/C in the range 174.0(8)–179.3(7)°).²⁰ The degree of closure of the N/C–Cu–C/N bond angles in compounds **I–VI** depends on the number of halogen atoms attached to copper and the strength of the Cu–X bond(s) formed. In general, the N/C–Cu–C/N angle decreases as the magnitude of the copper–halogen bonding increases. For example, the most closed angle observed, 119.9°, is for the one around Cu(1) in compound **V**, where there are two short Cu–I bonds completing tetrahedral coordination around copper. Further evidence for the strong copper–iodine bonding around Cu(1) comes from the weakening and consequent lengthening of the Cu–C/N bonds to 1.94(1) and 1.977(6) Å. In LT-CuCN, the Cu–C/N bond lengths lie in the range 1.84–1.87 Å.²⁰ It is also informative to compare compounds **V** and **VI** which both have frameworks with the same empirical formula, [Cu₂(CN)₂I][–], and contain tetrahedral and trigonal copper atoms. The tetrahedrally coordinated copper atoms have similar N/C–Cu–C/N bond angles of 119.9° (**V**) and 124.6° (**VI**). The differences between these angles can be accounted for by close examination of the Cu–I bond lengths. These are shorter around the tetrahedral copper site in **V** than in the corresponding sites in **VI**. Comparison of the corresponding trigonally coordinated copper atoms in **V** and **VI** is more complicated as there is

an additional interaction, a long Cu···C(3) interaction, which will also influence the N/C–Cu–C/N angle bending (137.0° (**V**) and 142.5° (**VI**)). Although this type of analysis works reasonably well and can be applied to all the compounds in this paper, it can only be approximate and is backward looking; the precise detail of the bending and twisting of the halogenocyanocuprate chains is a result of the requirement to create suitable cavities to accommodate the associated cations. The process is holistic; the degree of bending, the distribution of charge, and the linking and packing of chains do not occur as isolated steps but must occur in a concerted manner.

Conclusions

In this paper, we have demonstrated that LT-CuCN reacts easily at room temperature with a number of aqueous alkali-metal halide solutions (KX (X = Br and I) and CsX (X = Cl, Br and I)) to form a fascinating series of AX–CuCN addition products in which the –(CuCN)– chains present in CuCN itself are retained. The bending and twisting of the –(CuCN)– chains on coordination by halogen atoms generate a range of halogenocyanocuprate frameworks from open, zeolitic-like structures, in which hydrated alkali-metal cations reside in pores and channels, to interpenetrating chiral networks interleaved with anhydrous cations. For compounds with the same AX/CuCN ratio, although there is more than one possible structural solution involving different combinations of bends and twists of the halogenocyanocuprate chains, the particular structure adopted depends on the size of the alkali-metal cation. All of the addition products described here revert to CuCN on washing with removal of the A and X species from the structures. Why different ratios of the two different polymorphs of CuCN, LT- and HT-CuCN are recovered from different addition products is not yet known and will form the basis of future investigations along with studies of the reaction mechanisms. The hydrothermal method provides a route to single crystals of the simple AX–CuCN addition products. However, prolonged reaction under these conditions leads in some cases to further transformations. These include oxidation of some of the copper(I) to copper(II) to provide [Cu(H₂O)₄]²⁺ cations around which a further type of halogenocyanocuprate framework is assembled, and fragmentation of the –(CuCN)– chains to produce new types of structural building blocks. This paper shows that even simple looking systems can produce intriguing new materials with wide structural diversity.

Acknowledgment. A.M.C. thanks the Leverhulme Trust for a Research Fellowship. Mr. Alexander J. Freeborn, University of Reading, is thanked for assistance with the synthesis, and Dr. Andrew R. Cowley, University of Oxford, are also thanked for assistance with the synthesis and diffraction data collection, respectively.

Supporting Information Available: X-ray crystallographic files, in CIF format. This material is available free of charge via the Internet at <http://pubs.acs.org>.

IC049011+